Electronic Supplementary Material (ESI) for Journal of Materials Chemistry C.

Supporting Information for

TMC (TM = Co, Ni, Cu) Monolayers with Planar Pentacoordinate Carbon and Their Potential Applications

Changyan Zhu,[a] Haifeng Lv,[b] Xin Qu,[c] Min Zhang,*[a] Jianyun Wang,[c] Shizheng Wen,[f] Quan Li,[c]

Yun Geng,[a] Zhongmin Su,[ae] Xiaojun Wu,*[b] Yafei Li,*[d] Yanming Ma[c]

[a.] *Institute of Functional Material Chemistry, Faculty of Chemistry & National & Local United Engineering Laboratory for Power Battery, Northeast Normal University, Changchun 130024, China*

[b.] *CAS Key Laboratory of Materials for Energy Conversion, School of Chemistry and Materials Sciences, CAS Center for Excellence in Nanoscience, and Hefei National Laboratory of Physical Sciences at the Microscale, University of Science and Technology of China, Hefei, Anhui 230026, China*

[c.] *State Key Laboratory of Superhard Materials, College of Physics, Jilin University, Changchun 130024, China*

[d.] *Jiangsu Collaborative Innovation Centre of Biomedical Functional Materials, Jiangsu Key Laboratory of New Power Batteries, School of Chemistry and Materials Science, Nanjing Normal University, Nanjing 210023, China*

[e.] *School of Chemistry and Environmental Engineering, Changchun University of Science and Technology, Changchun 130024, China*

[f.] *Jiangsu Province Key Laboratory of Modern Measurement Technology and Intelligent Systems, School of Physics and Electronic Electrical Engineering, Huaiyin Normal University, Huaian 223000, China*

Documented error estimates here are important to avoid future confusion between theoretical data and experimental data. Hence, the experimentally prepared 3D Ni_3C crystal is optimized at current computational level. The lattice parameters *a, b, c* and the Ni-C bonding length in experiment and theory, as well as the error are summarized in Table S0. It is clearly that the error is only ~1.0%. According to the documented error estimates for 3D Ni_3C crystal, we deduce that the optimized lattice parameters and the TM-C, C-C bonding lengths in TMC monolayers will fluctuate during ±1.0%.

Meanwhile, the van-der-Waals (vdW) interaction cannot be described properly due to the deficiency of used approximate exchange-correlation functional in DFT. Hence, the DFT-D3 approach containing the vdW interaction was employed to re-optimize the TMC monolayers and LiC monolayers. The optimized lattice parameters *a* and *b*, and the lengths of C-C, TM-TM and TM-C bonds DFT functional and dispersion-corrected F are summarized in Table S1. According to these data, it is apparent that optimized geometry is little difference using two computational functionals, which shows very weak long-range interaction in our systems. In addition, their cohesive energies and formation energies are also calculated under DFT-D3 functional, shown in Table S3. Compared with the results using PBE functional, the largest difference in cohesive energy is 0.16 eV/atom for Cu_2Si monolayer, which is within acceptable error range. However, the absolute error in formation energy between PBE functional and DFT-D3 functional is at the similar level (less than 0.19 eV/atom), except Cu-containing monolayers (0.33 eV/atom) because the energy of bulk Cu is more sensitive to the vdW interaction (the absolute energy for bulk Cu is -14.91345722 eV using PBE functional, while the absolute energy for bulk Cu is -17.60916404 eV using DFT-D3 functional).

Table S1. Lattice parameters *a, b, c* and the Ni-C bonding length of Ni_3C crystal in experiment and theory, as well as the error.

Ni_3C	Experimental	Theoretical	Error
a	4.553 Å	4.596 Å	0.944%
b	4.553 Å	4.596 Å	0.944%
c	12.920 Å	12.992 Å	0.557%
R_{Ni-C}	1.861 Å	1.884 Å	1.473%

Table S2. Optimized lattice parameters *a* and *b*, and lengths of the C-C, TM-TM and TM-C bonds using DFT functional and dispersion-corrected DFT-D3 functional. The parameters using DFT-3D functional are in parentheses.

Length(Å)	a	b	R_{C-C}	R_{TM-TM}	R_{TM-C}
α- CoC	7.08(7.07)	3.73(3.73)	1.48(1.48)	2.32-2.36(2.31-2.34)	1.88-1.95(1.91-1.94)
β-CoC	4.49(4,48)	5.92(5.91)	1.48(1.48)	2.31-2.39(2.31-2.39)	1.91-1.92(1.91-1.92)
α- NiC	7.20(7.19)	3.77(3.76)	1.38(1.38)	2.33-2.36(2.32-2.35)	1.95-2.01(1.95-2.01)
β-NiC	4.46(4.46)	6.04(6.03)	1.39(1.40)	2.33-2.34(2.32-2.33)	1.93-1.98(1.92-1.98)
α- CuC	7.52(7.49)	3.97(3.94)	1.30(1.30)	2.40-2.47(2.39-2.46)	2.04-2.21(2.03-2.18)
β-CuC	4.61(4.60)	6.45(6.40)	1.30(1.30)	2.36-2.46(2.35-2.45)	2.03-2.15(2.02-2.12)
α- LiC	7.85(7.81)	4.10(4.08)	1.26(1.26)	2.48-2.62(2.47-2.61)	2.15-2.23(2.15-2.21)
β-LiC	4.88(4.86)	6.61(6.56)	1.26(1.26)	2.37-2.62(2.34-2.61)	2.16-2.22(2.15-2.20)

Table S3. Cohesive energy and formation energy of different species using DFT-D3 functional.

Species	E_{coh}/E_f(eV/atom)	Species	E_{coh}/E_f(eV/atom)
α-CoC	6.10/0.81	α-LiC	4.69/0.0.17
β-CoC	6.09/0.82	β-LiC	4.68/0.17
α-NiC	5.94/0.78	Graphene	8.04/0.00
β-NiC	5.93/0.79	Ti_2C	6.39/0.23
α-CuC	5.12/0.97	TiC_3	6.94/0.57
β-CuC	5.11/0.99	Cu_2Si	3.61/0.51

Table S4. Relative energies (meV/TM_4C_4) among nonmagnetic (NM), ferromagnetic (FM), and three antiferromagnetic (AFM-a, AFM-b and AFM-c) states for TMC monolayers at the PBE functional level.

System	NM	FM	AFM-a	AFM-b	AFM-c
α-CoC	13.93	0.23	13.92	0.00	13.93
β-CoC	165.73	117.88	165.73	165.73	0.00
α-NiC	41.38	0.00	40.72	41.40	41.38
β-NiC	9.31	0.00	9.31	9.32	9.31
α-CuC	0.00	0.02	0.02	0.02	0.02
β-CuC	0.00	0.02	0.03	0.03	0.02

Table S5. Relative energies (meV/TM_4C_4) among nonmagnetic (NM), ferromagnetic (FM), and three antiferromagnetic (AFM-a, AFM-b and AFM-c) states for CoC and NiC monolayers at the hybrid HSE06 functional level.

System	NM	FM	AFM-a	AFM-b	AFM-c
α-CoC	2463.30	2122.45	1274.02	0.00	387.95
β-CoC	2432.48	952.93	707.21	570.58	0.00
α-NiC	179.18	0.00	41.17	50.05	169.37
β-NiC	159.34	0.00	59.39	159.95	115.21

Table S6. Types of the ground states (GS) for CoC and NiC monolayers and their magnetic moments (M, μB) on different atoms.

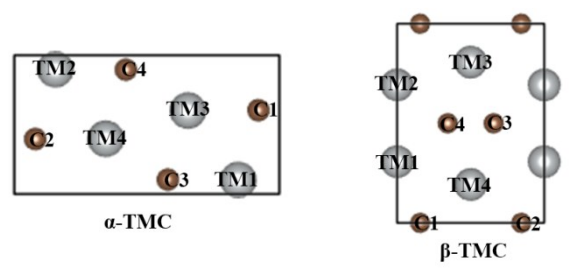

System	GS	M-TM1	M-TM2	M-TM3	M-TM4	M-C1	M-C2	M-C3	M-C4
α-CoC	AFM-b	1.38	1.38	1.42	1.42	0.05	0.05	0.05	0.05
β-CoC	AFM-c	1.61	1.61	1.61	1.61	0.00	0.00	0.00	0.00
α-NiC	FM	0.42	0.42	0.45	0.45	0.06	0.06	0.06	0.06
β-NiC	FM	0.12	0.12	0.41	0.41	0.02	0.02	0.07	0.07

Table S7. Magnetic anisotropic energies of α-CoC, β-CoC, α-NiC and β-NiC monolayers in the unit of μeV per TM atom. The easy axis (EA) is the (100) direction for α-CoC monolayer and the EA is the (010) direction for β-CoC, α-NiC and β-NiC monolayers.

μeV/TM	**001-100**	**010-100**	**110-100**	**111-100**
α-CoC	3685	832	545	1651
μeV/TM	**001-010**	**100-010**	**110-010**	**111-010**
β-CoC	1691	320	216	754
α-NiC	863	225	166	451
β-NiC	430	141	107	260

Table S8. Elastic constants (C_{11}, C_{22}, C_{12}, C_{21}, C_{66}) in the unit of N/m, Young's modulus (Y_a and Y_b) in the unit of N/m and Poisson's ratios (ν_a, ν_b).

	C_{11}	C_{22}	C_{12}	C_{21}	C_{66}	Y_a	Y_b	ν_a	ν_b
α-CoC	228.84	197.24	85.45	85.45	80.26	191.82	165.33	0.43	0.37
β-CoC	239.17	199.34	65.10	65.10	63.74	217.91	181.62	0.33	0.27
α-NiC	181.35	162.61	73.06	73.06	60.12	148.52	133.18	0.45	0.40
β-NiC	217.26	181.28	56.89	56.89	49.93	199.41	166.38	0.31	0.26
α-CuC	109.10	97.97	51.68	51.68	35.99	81.84	73.49	0.53	0.47
β-CuC	136.84	102.90	44.11	44.11	26.72	117.93	88.68	0.43	0.32

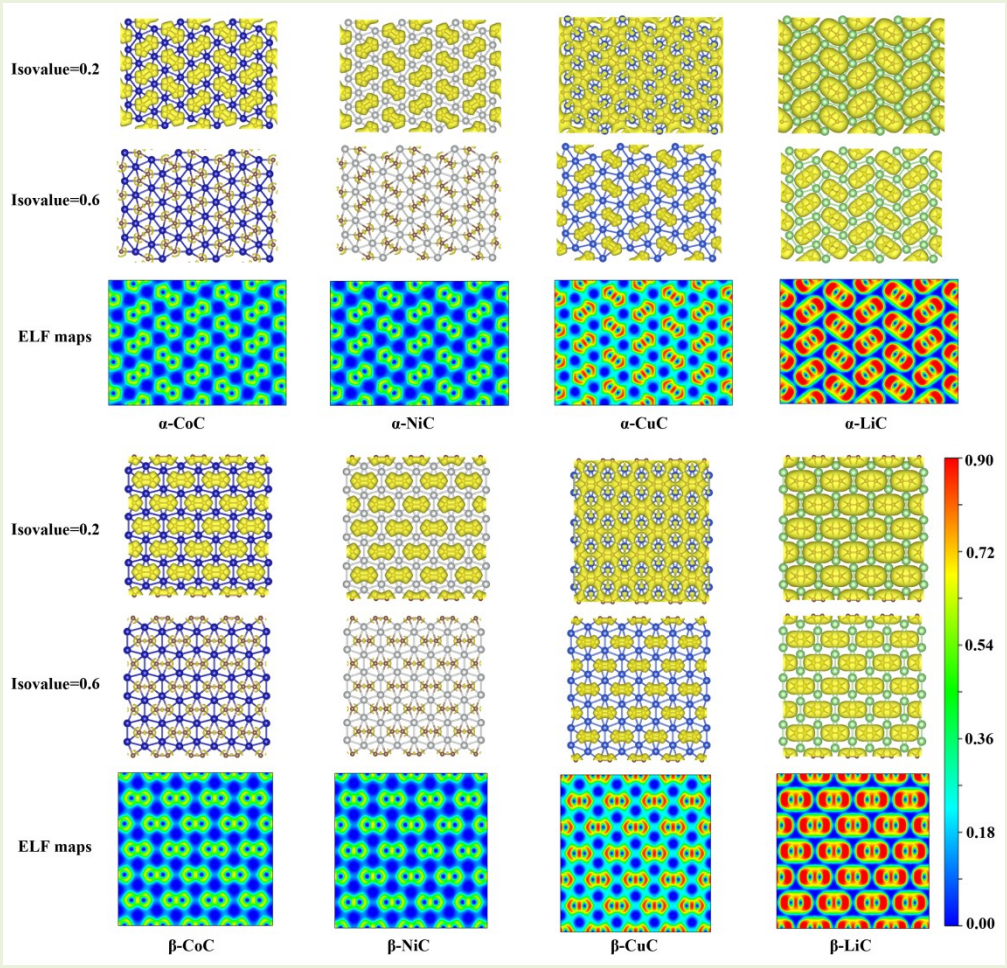

Figure S1. Isosurfaces of electron localization function (ELF) and the ELF maps sliced in (001) direction for TMC monolayers and LiC monolayers. In the ELF maps, the red and blue colours refer to the highest value (0.90) and the lowest value (0.00) of ELF, indicating accumulation and depletion of electrons at different coloured regions, respectively.

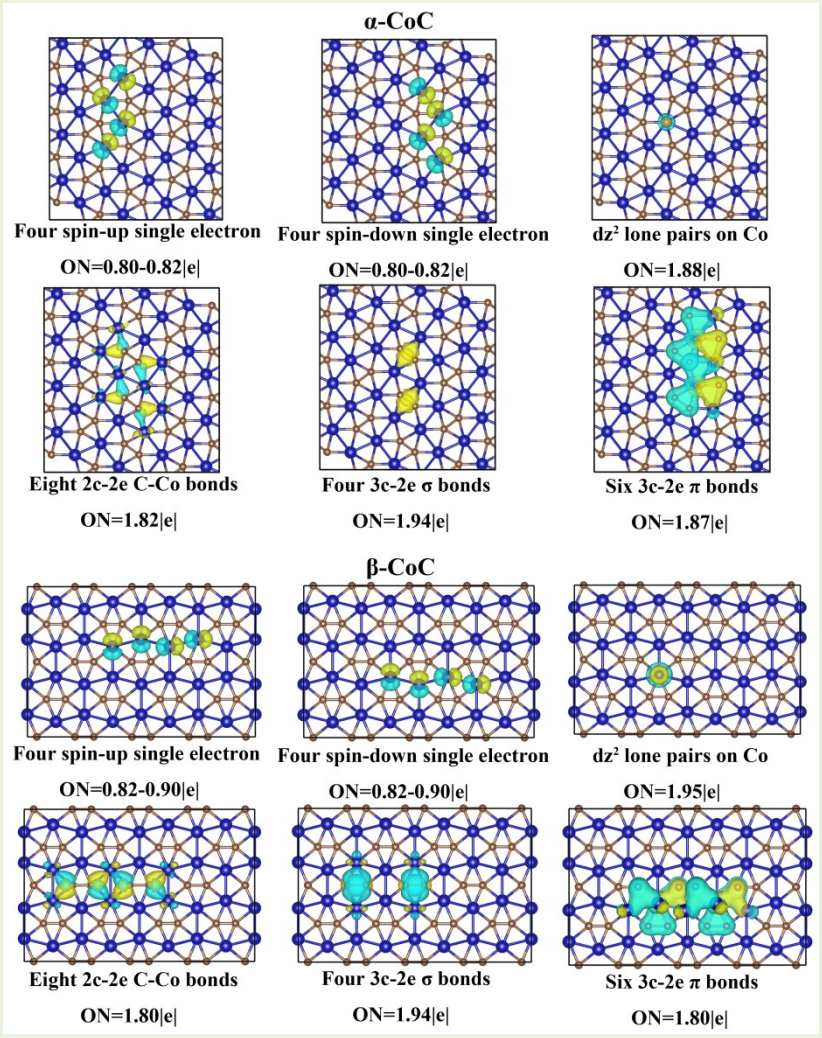

Figure S2. SSAdNDP bonding patterns of CoC monolayers. ON is short for occupation number.

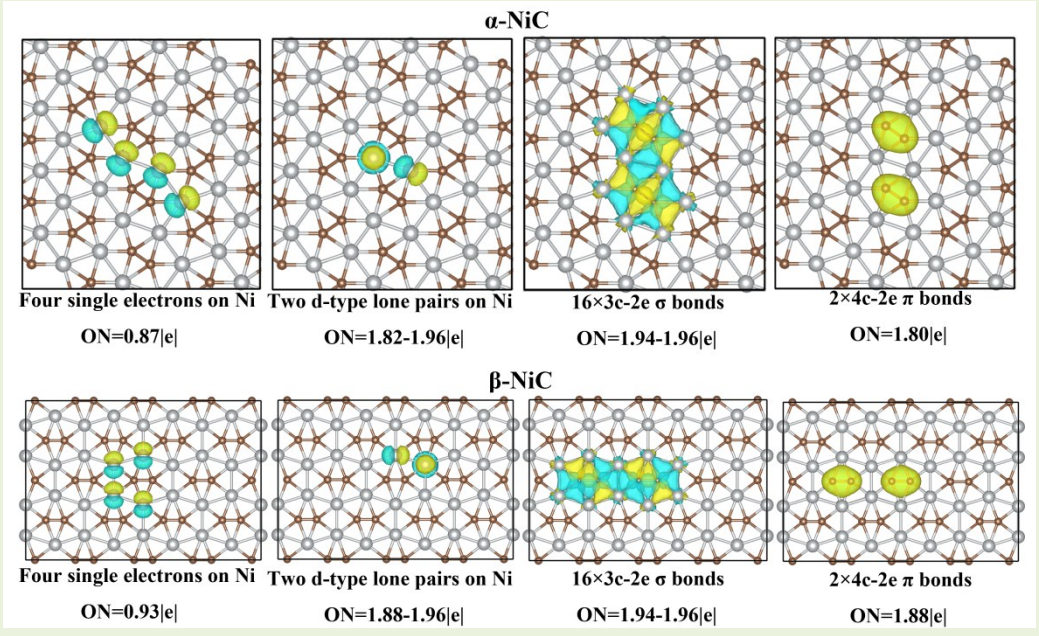

Figure S3. SSAdNDP bonding patterns of NiC monolayers. ON is short for occupation number.

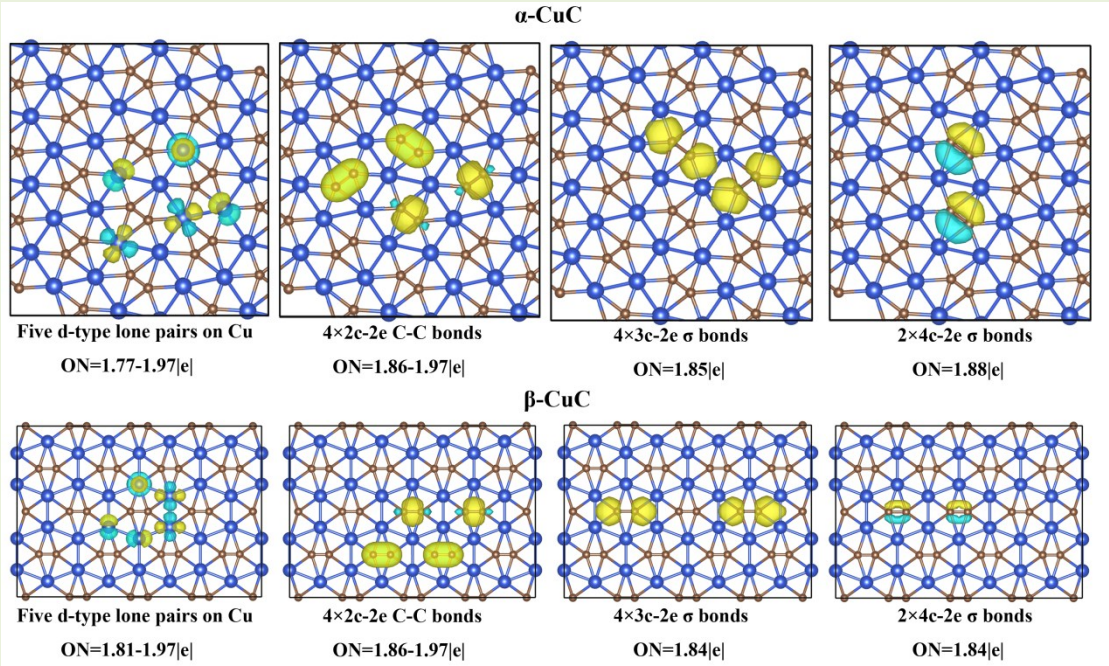

Figure S4. SSAdNDP bonding patterns of CuC monolayers. ON is short for occupation number.

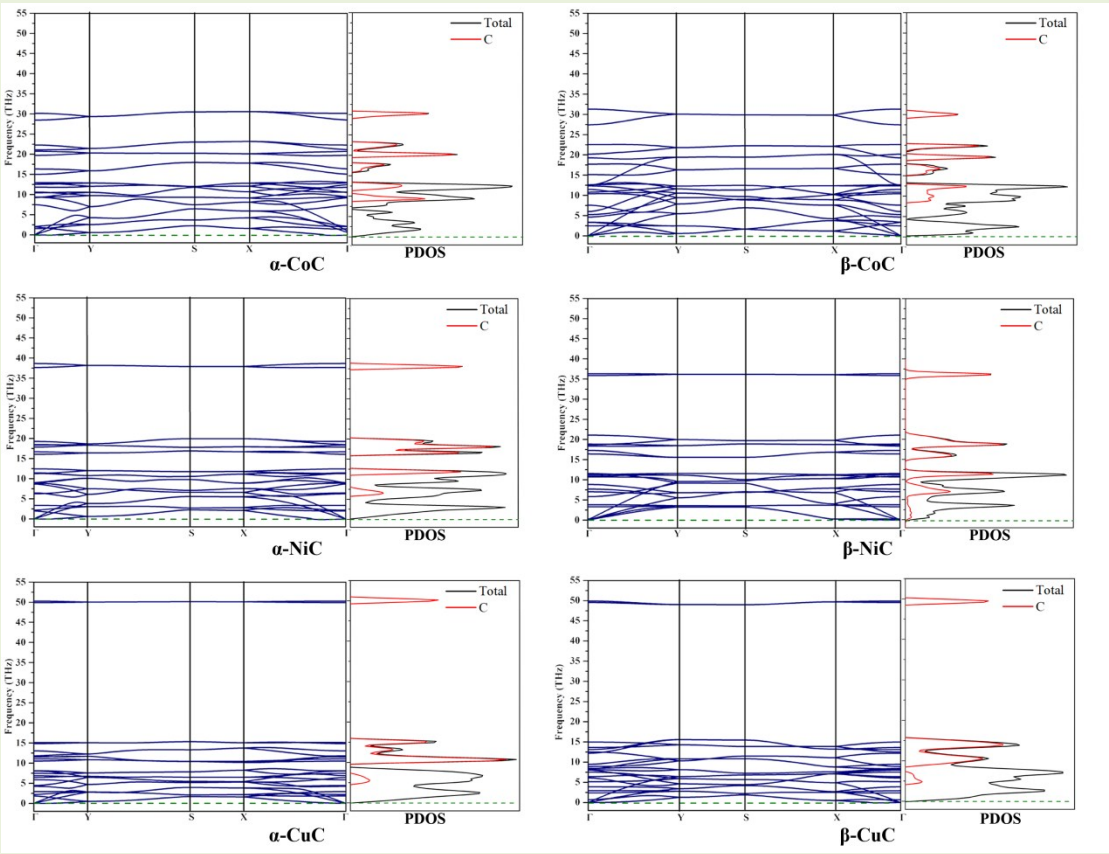

Figure S5. Phonon dispersion and phonon density of states (PDOS) of TMC monolayers computed using the PBE functional.

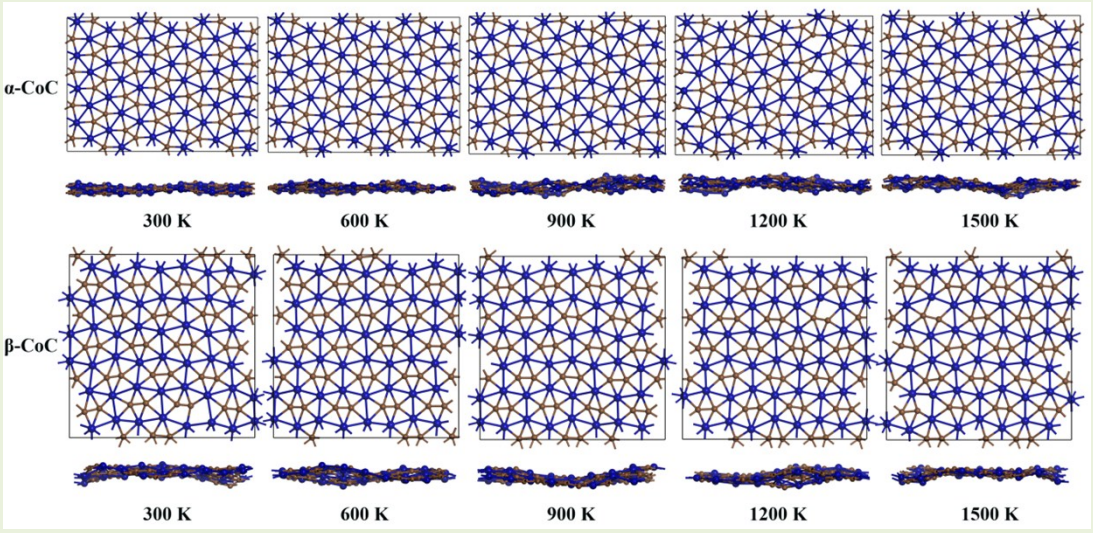

Figure S6. Snapshots of CoC monolayers equilibrium structures at 300 K, 600 K, 900 K, 1200 K, 1500 K at the end of 10 ps AIMD simulations.

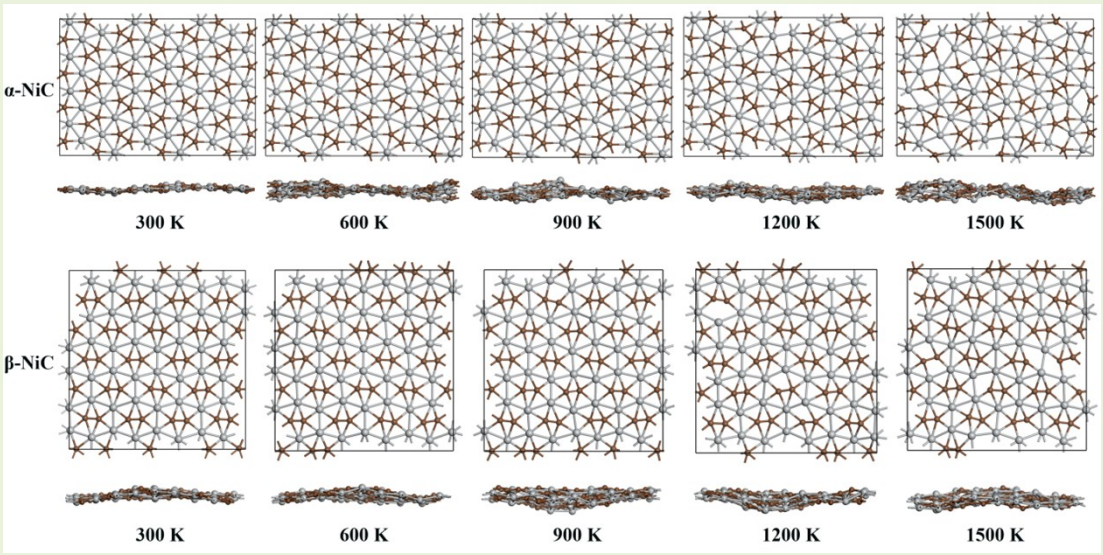

Figure S7. Snapshots of NiC monolayers equilibrium structures at 300 K, 600 K, 900 K, 1200 K, 1500 K at the end of 10 ps AIMD simulations.

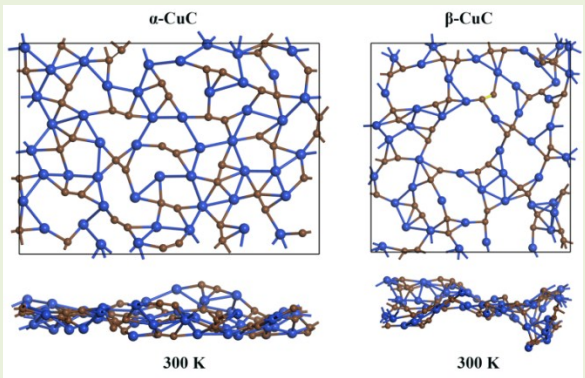

Figure S8. Snapshots of CuC monolayers equilibrium structures at 300 K at the end of 10 ps AIMD simulations.

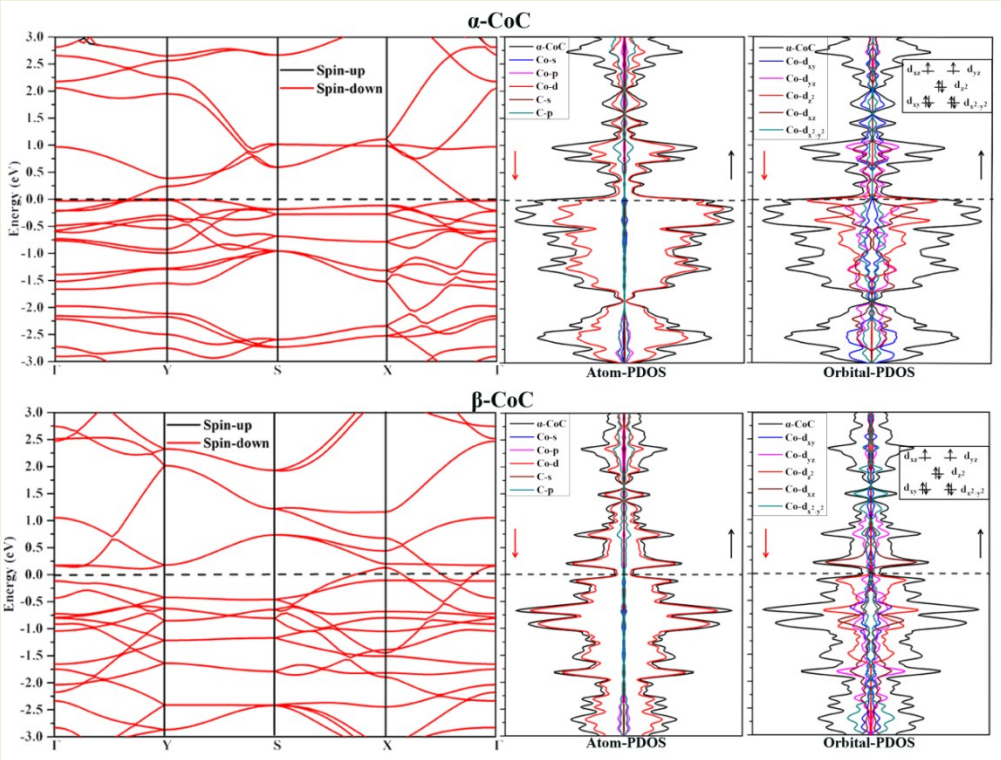

Figure S9. Electronic band structure, atom-projected and orbital-projected densities of states for CoC monolayers using the PBE functional. Dashed lines refer to the Fermi level set to zero.

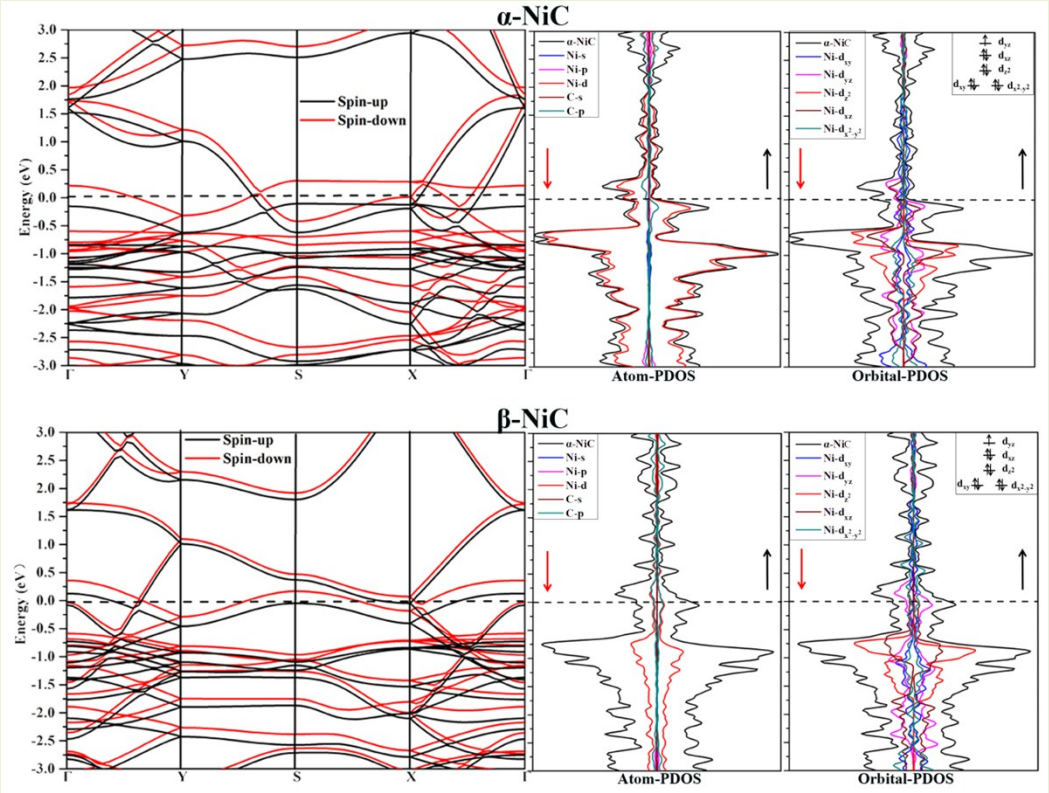

Figure S10. Electronic band structure, atom-projected and orbital-projected densities of states for NiC monolayers using the PBE functional. Dashed lines refer to the Fermi level set to zero.

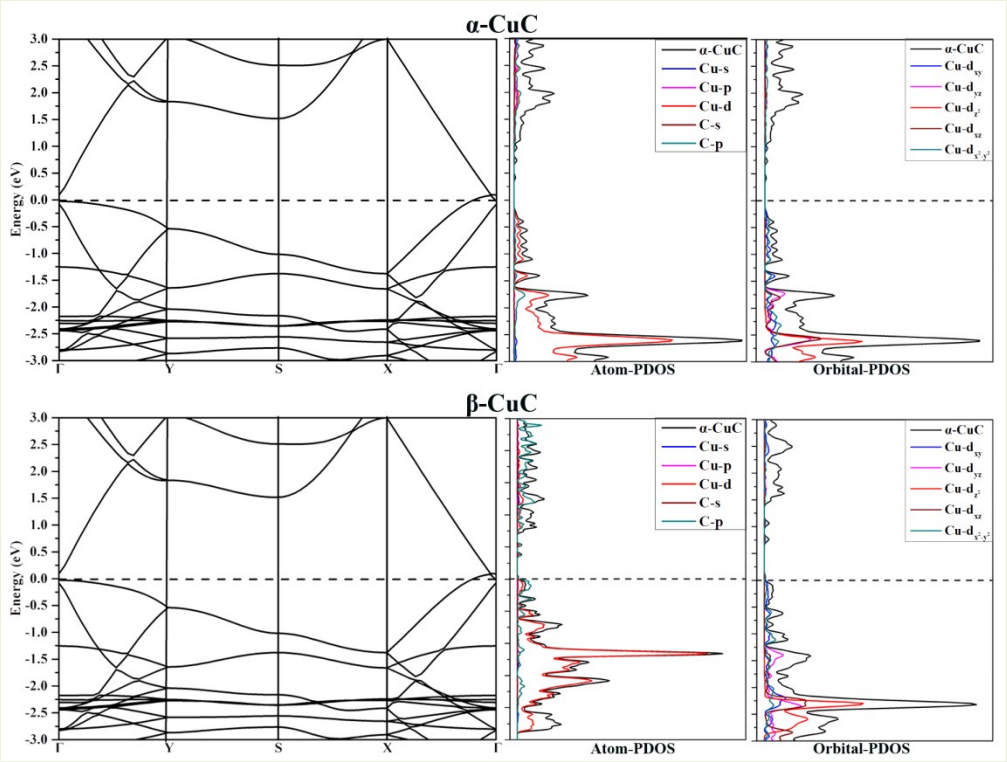

Figure S11. Electronic band structure, atom-projected and orbital-projected densities of states for CuC monolayers using the PBE functional. Dashed lines refer to the Fermi level set to zero.